JOURNAL OF MATERIALS SCIENCE **34** (1999) 349–353

A versatile plasma technique to improve plastic materials against gas and water-vapour permeation

E. M. MOSER*, C. MÜLLER
Swiss Federal Laboratories for Materials Testing and Research EMPA, CH-9014 St Gallen, Switzerland
E-mail: eva.moser@empa.ch

Plasma-enhanced chemical deposition processes have been studied by comparing the performance of flexible diffusion barrier layers on plastic films produced in the same reactor. Under similar experimental conditions, a higher deposition rate is achieved by microwave discharges than by bipolar, pulsed d.c. magnetron sputtering processes. However, with both discharge modes, dense hydrocarbon coatings were produced, exhibiting a barrier improvement factor up to 120 and a flexibility ranging from 1.1%–8.8% before formation of microcracks started to dominate permeation characteristics. The density of the coatings is 1.0–1.6 g cm^{-3} and their hydrogen content varies from 23%–33%.

1. Introduction

Storing food, drugs, delicate materials and microelectronic items against environmental influences over a long period of time is a vital problem of our time. New materials or methods for improving existing materials against permeation of gas, water vapour, and substances have to be found to achieve this goal. The conversion of lightweight plastic films into packaging media of high functionality is already being considered as a substitute for the metal and glass counterparts. In terms of environmental aspects, the chemically inert and transparent polyethylene terephthalate (PET), and similar plastic films, are now widely used. When destroyed by heat, they do not evolve toxic vapours. These properties do not yet fulfil the above mentioned criteria. Laminated structures with several layers of polymeric materials (e.g. EVOH) have been used to compensate for the lower performance in either gas or water permeation [1]. In addition, plastic films have been coated with thin barrier layers consisting of selected metals or metal oxides. All these coatings should be thin, elastic, free from pinholes and microcracks, and they should not lose their ability to prevent permeation during storage time. Metal oxide barrier layers are optically transparent, microwaveable, and meet the ecological demands but their application range is limited due to their intrinsic rigidity [2, 3]. Plasma-polymerized coatings of hydrocarbon and monomers containing a source of fluorine and sulphur atoms have reduced solvent permeation in plastic containers [4, 5]. Furthermore, multilayer systems composed of oxide-like barrier layers embedded in polymer-like material have been developed [6]. However, thin hydrocarbon barrier layers proved to be a good alternative to the rigid metal oxide barrier layers [7, 8]. In this work, we directly compared the properties of hydrocarbon coatings deposited on to PET films by bipolar, pulsed d.c. magnetron sputtering processes and microwave discharges under similar experimental conditions.

2. Experimental procedure

A versatile low-temperature plasma-enhanced chemical vapour deposition reactor was set up, which permitted the following treatments to be carried out using variable mixtures of gases, flow rates and working pressures, i.e. varying known and proven plasma technique parameters: treatment by microwave discharges (MW, 2.448 GHz), radiofrequency (r.f., 13.56 MHz), and direct current (d.c.) sputtering by circular magnetrons, while biasing the sample by r.f., d.c., or earthing (Fig. 1). The complete installation was controlled by an universal electronic system in which all energy generators worked in variable controllable modes and were equipped with a power supply for generating pulsed and non-pulsed operating modes.

The starting pressure in the reactor was $\sim 10^{-6}$ mbar. After optimization, the experimental parameters were set to a MW/d.c. input power of 100 or 200 W, respectively. In the case of d.c. magnetron sputtering processes, a pulse frequency of 25 kHz, a reverse voltage of 15% of the operating d.c. input voltage, and a reverse recovery time of 2 μs were chosen, whereas microwave discharges were performed in continuous mode by monitoring MW input power and frequency. The target consisted of a circular hot-pressed carbon

* Author to whom all correspondence should be addressed. EMPA, CH-9014 St. Gallen, Switzerland.

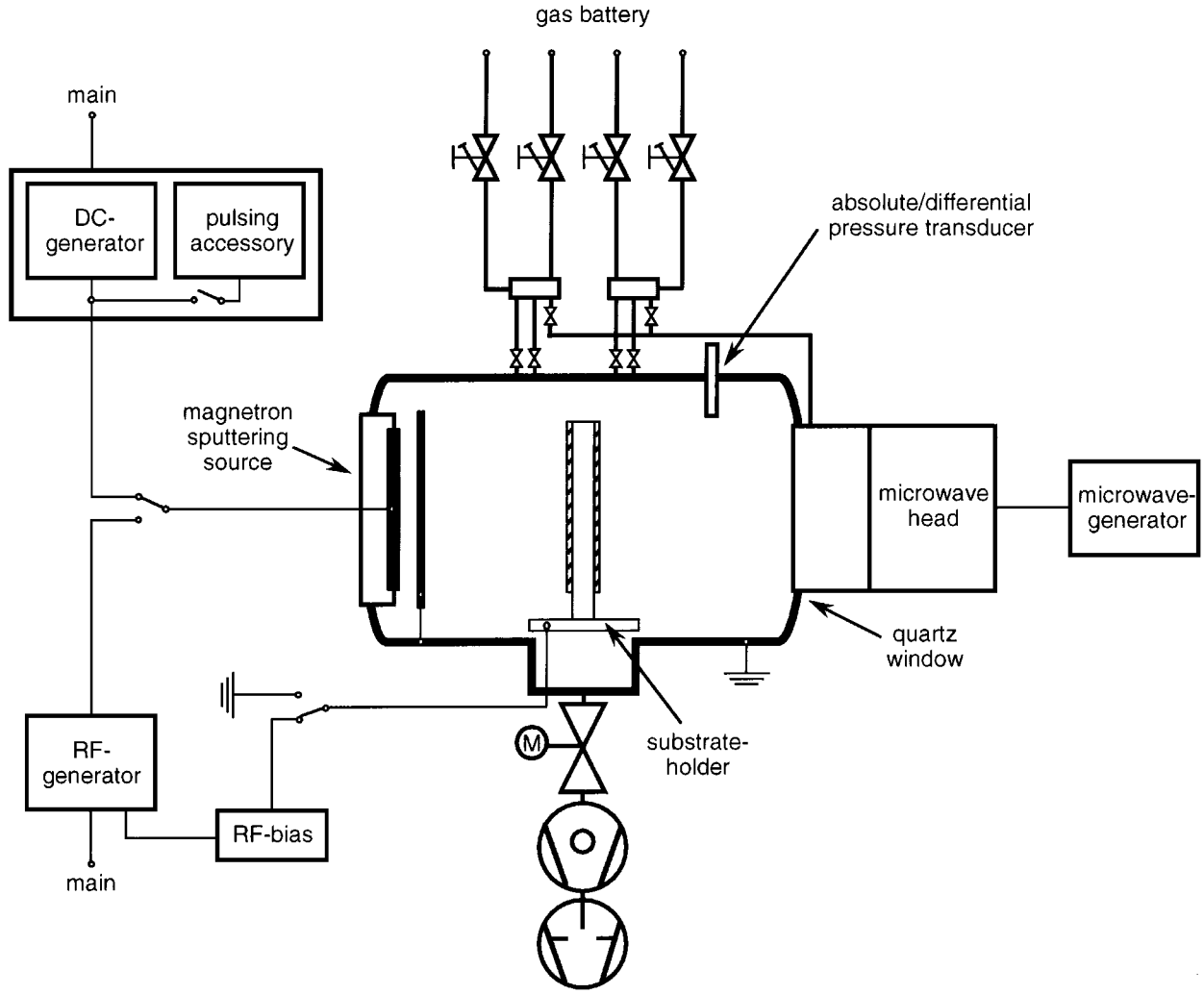

Figure 1 Schematic drawing of the plasma-enhanced chemical vapour deposition reactor.

disc (purity 99.999%), 6.3 mm thick, bonded to a copper plate.

For non-reactive d.c. sputtering processes (coatings A), the deposition time was 10 min, 2 min for reactive gas mixtures (coatings B and C) and 1 min for MW-activated processes (coatings D). The working pressure was regulated by a butterfly valve connected to a baratron gauge.

The samples were either connected to earth or were biased by a capacitively coupled radio frequency ($V_b = -40$ or -90 V). The substrate temperature was measured by a thermocouple attached to the sample holder surface. The temperature ranged from room temperature (23 °C) to a maximum value of 29 °C for extreme conditions (200 W MW power). Polythylene terephthalate (PET) film, DuPont-MYLAR® type A, with a thickness of 12 μm and a piece of silicon wafer [1 0 0] placed adjacent to the PET-film were used as substrates.

Oxygen permeability was measured at 0% relative humidity, 23 °C, according to ASTM D 3985-81, using a Mocon OX-TRAN 2/20 instrument. Water-vapour transmission measurements were conducted with a Lyssy Vapour Permeation Tester L 80-4000. Total luminous transmittance of the coated and untreated PET films was investigated according to ASTM D 10003-92 (CIE: Y-value, 10 °, D65).

Coating thickness was determined by profilometry (Tencor P10) on pieces of silicon wafer. The hydrogen content, possible impurities, and the density of coatings were analysed on coated Si[1 0 0] substrates using Rutherford backscattering (RBS), elastic recoil detection analysis (ERDA), and X-ray photoelectron spectroscopy (XPS). Internal tension of the coated PET-films was investigated by evaluation of curvature.

Stretching of the coated films allowed the analysis of their elastic behaviour by a method based on interferometry. The technique developed at EMPA will be described in more detail elsewhere [9]. Microcrack formation on the elongated sample and its influence on diffusion barrier properties was established by the combination of scanning electron microscopy and permeability measurements. After having etched the PET samples with 80% sulphuric acid, coating defects were investigated. The AFM images of the substrate and the coated PET films were captured under ambient conditions using a Bioscope-AFM (Digital Instruments) and an Explorer-AFM (TopoMetrix, Model TMX 2000) in tapping mode and non-contact mode of operation, respectively.

All tests were compared with a dummy film from the same batch of material. A periodic inspection study of the diffusion property of a carefully stored sample

TABLE I Summary of properties of amorphous hydrocarbon films

Sample	Power	Bias	Thickness[a] (nm)	OXTR[a] (cm^3 (m^2 d bar)$^{-1}$)	BIF[b]	Elongation (%)	Water[c] (g m^{-2} d^{-1})	ρ_M[d] (g m^{-3})	ρ_N[e] (g at cm^{-3})	H-cont.[f]	Transm.[g]
A1	100	Earth	20 ± 2	2.2 ± 0.1	56	2.5 ± 0.2	0.6 ± 0.1	1.58	0.194	0.35	63
A2	100	r.f.-ind.	21 ± 2	24.2 ± 0.2	5		14.0 ± 0.2				64
A3	200	Earth	31 ± 1	1.0 ± 0.1	124	2.0 ± 0.2	0.4 ± 0.1				64
B1	100	Earth	27 ± 2	55.2 ± 0.2	2	5.8 ± 0.2		1.35	0.155	0.30	86
B2	100	r.f.-ind.	58 ± 3	2.7 ± 0.1	46	2.8 ± 0.2	0.3 ± 0.1	1.21	0.159	0.40	75
B3	100	Earth	35 ± 2	55.4 ± 0.2	2	8.8 ± 0.2		1.03	0.158	0.50	83
B4	200	r.f.-ind.	75 ± 3	2.4 ± 0.1	52	2.8 ± 0.2	0.4 ± 0.1	1.36	0.169	0.36	77
C1	100	Earth	46 ± 3	14.2 ± 0.2	9	4.9 ± 0.2	14.2 ± 0.2	1.22	0.173	0.45	86
C2	100	r.f.-ind.	76 ± 3	1.1 ± 0.1	112	2.8 ± 0.2	0.4 ± 0.1	1.46	0.207	0.45	77
D1	100	Earth	91 ± 3	102.1 ± 0.2	1	2.3 ± 0.2	16.5 ± 0.2	1.15	0.137	0.33	82
D2	100	r.f.-ind.	97 ± 3	9.3 ± 0.1	13	2.7 ± 0.2	2.0 ± 0.1	1.47	0.212	0.46	72
D3	100	Earth	141 ± 4	1.1 ± 0.1	112	1.1 ± 0.2	0.1 ± 0.1	1.39	0.210	0.49	76
D4	100	r.f.-ind.	134 ± 5	1.1 ± 0.1	112	1.7 ± 0.2	0.2 ± 0.1	1.44	0.204	0.45	74
PET			12 μm	123.9 ± 0.1	–		20.4 ± 0.2				89
SiO_x			36 ± 4	2.7 ± 0.1	46	1.7 ± 0.2	0.9 ± 0.1				84

[a] Oxygen permeability.
[b] Barrier improvement factor: untreated/treated film.
[c] Water vapour permeability.
[d] Mass density.
[e] Gram atom number density.
[f] Atomic fraction of hydrogen [C_1H_x].
[g] Total luminous transmittance (Y-value: CIE).

(23 °C, 0% relative humidity) was undertaken in order to analyse long-term behaviour.

3. Results

3.1. Magnetron sputtering deposition

Fig. 2a and b show plots of coating thickness of samples prepared at the same deposition time and oxygen permeation versus d.c. input power, respectively. Coating thickness increases with power for both pulsed and non-pulsed modes of operation. With increasing power, oxygen permeation increases for the non-pulsed coatings, whereas for pulsed coatings best barrier properties with an improvement factor of about 120 are achieved at 200 W d.c. input power.

The optimal pressure for this process is between 2 and 5×10^{-3} mbar. In this range almost no internal tensions of the coatings arise. The coatings are homogeneous over a diameter of about 120 mm even under the variation of the working distance between 80 and 160 mm. The coatings were observed to be slightly brownish but the general transparency is acceptable for specific industrial applications.

Table I presents the properties of the coatings (A–C) produced by bipolarly pulsed d.c. magnetron processes. The barrier improvement factor for oxygen (BIF) is independent of the substrate thickness and its permeability and is a function of the coating defect parameters. A correlation with the water vapour data is observed. So far, an elongation value of more than 5% has been achieved for coatings with lower permeation performance.

Although the deposition rate of the processes described could not be increased by pulsing d.c. magnetron discharges, a significant improvement of the barrier layer results, as already described elsewhere [7]. The same performance properties as summarized in Table I were obtained for coated samples stored for 6 months at defined conditions.

3.2. Microwave discharge deposition

In the same reactor under similar experimental conditions as used for d.c. magnetron sputtering processes, hydrocarbon films were deposited on PET films by

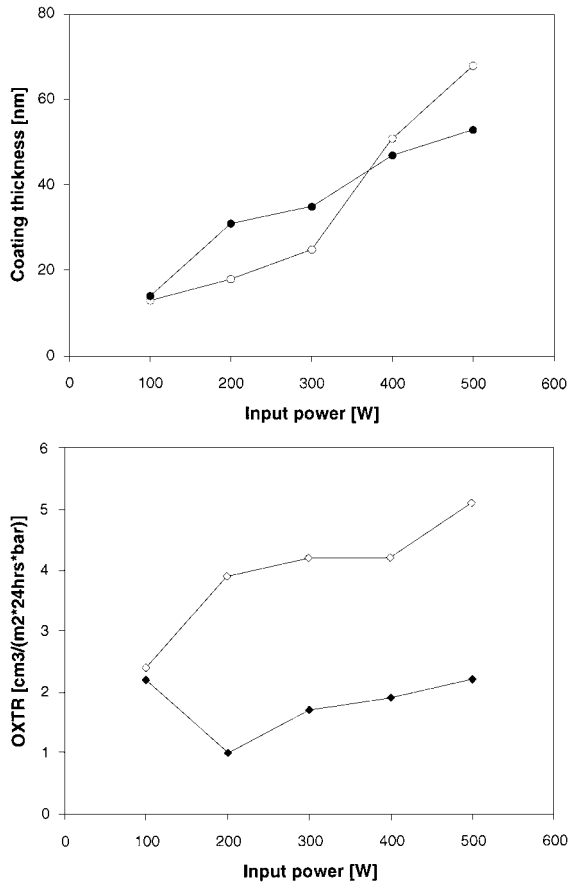

Figure 2 Characteristics of hydrocarbon layers (performed by d.c. magnetron sputtering in an argon plasma) as a function of d.c. input power in (●, ◆) pulsed mode and in (○, ◇) non-pulsed mode. (a) Coating thickness (nm), (b) oxygen permeability (cm^3 ($m^2 \cdot d \cdot bar$)$^{-1}$).

microwave discharges. For MW processes, the deposition rate is increased by a factor of eight (coating D3 compared to coating B3), taking into account the different deposition time. If the gas flow is increased, the functional performance and the deposition rate of the MW coatings (D1–D4) are improved, in contrast to the d.c. coatings (B1–B4).

In Fig. 3a, the AFM image of an untreated PET-film reveals a morphology consisting of 10–20 nm sized grains and an RMS roughness of about 0.8 nm. All investigated coatings show a very homogeneous morphology with an RMS roughness of 1.5–2.5 nm and a grain size of 20–40 nm. The structure of the films is very similar and depends neither on the discharge mode, nor on the deposition parameters. The grain size of the MW-coated PET film (D4, Fig. 3c) is slightly enhanced compared to the d.c. coating (C2, Fig. 3b), which is most probably due to the higher coating thickness. In the 20 μm micrometre scale, an unidirectional orientation of the biaxially stretched PET substrate with an RMS roughness of 11–22 nm is observed. The oriented mounds on the substrate surface have also been found in the coated PET films and have been confirmed using SEM.

3.3. Influence of r.f. biasing

The samples were either earth biased or the radiofrequency was capacitively coupled to the substrate holder. Because of the negative potential on the substrate, ions are accelerated in the sheath towards the substrate, impinging on it with a higher energy. The density of the coatings (C2, D2, and D4) is expected to be higher and the permeability values to be lower. However, the flexibility of the coatings decreases with increasing density for d.c. discharge mode. In addition, the deposition rate is increased by applying r.f. biasing. As far as MW coatings are concerned, r.f. bias has a positive effect on the properties of the samples (D2, D4).

The permeability of the r.f.-biased sample A2 is significantly increased compared to sample A1. Here, the equilibrium of ion bombardment controlled by the plasma potential and the negative bias voltage at the film surface seems to be negatively influenced by etching processes of the substrate surface. As a result, more pinholes were observed in sample A2 than in A1.

4. Discussion

Under similar experimental conditions, microwave discharge processes lead to a faster film growth which is most probably due to the relatively highly dissociated plasma conditions [10]. Additional work is required to elucidate the process parameters for optimal mechanical and chemical properties in order to fulfil the required functional performances. Because the coatings showing good diffusion barrier properties are characterized by a gram atom number density higher than 0.2 g at cm^{-3}, we prefer to describe the developed coatings as dense hydrocarbon films, according to Angus [11].

The reduction in permeation is limited by the transport through coating defects, such as pinholes, grain boundaries or microcracks [3]. So far, AFM and TEM [7] investigations of the presented samples have

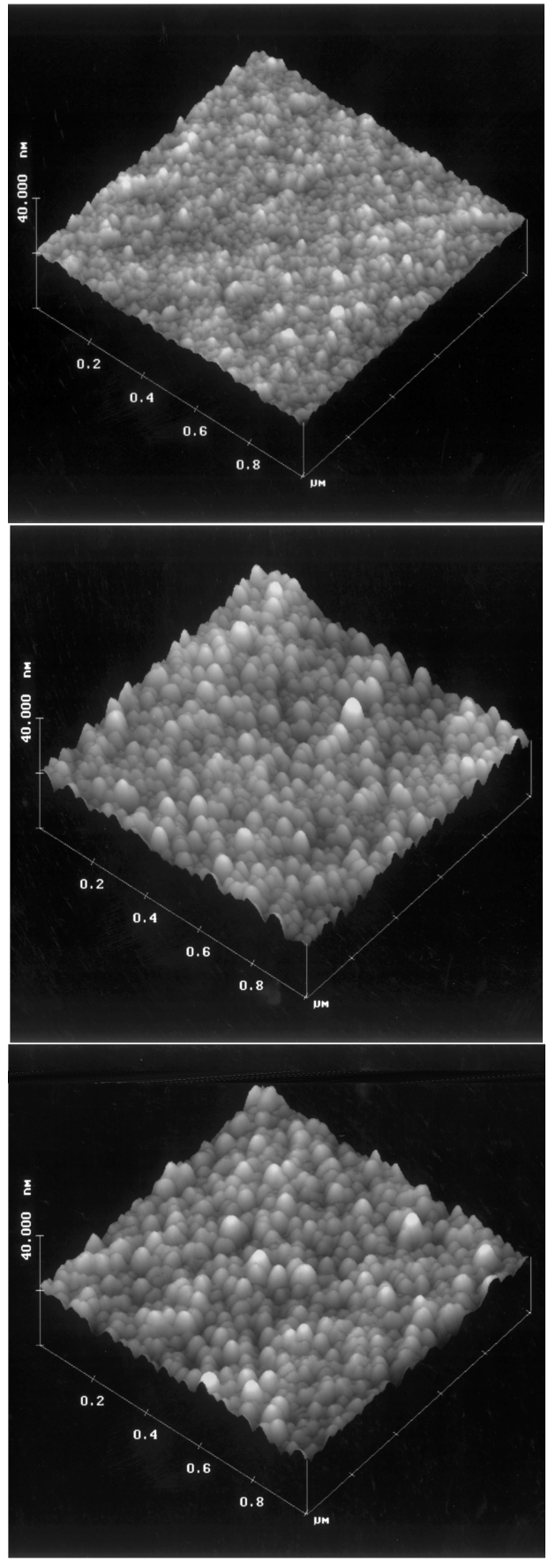

Figure 3 AFM images show topography of PET substrate and hydrocarbon layers. (a) Uncoated PET (reference; 1000 × 1000 nm, 0–40 nm vertical scale, grain size 10–20 nm, RMS roughness 0.8 nm). (b) 76 nm thick C:H layer on PET (C2, 100 W d.c.; biased; 1000 × 1000 nm, 0–40 nm vertical scale, grain size 25–35 nm, RMS roughness 2.0 nm). (c) 134 nm thick C:H layer on PET (D4, 100 W MW; biased; 1000 × 1000 nm, 0–40 nm vertical scale, grain size 30–40 nm, RMS roughness 1.5 nm).

revealed a very homogenous morphology for the coatings with an RMS roughness of about 2 nm and a grain size of about 30 nm on a unidirectional structured PET film. The anisotropy of the biaxially stretched substrate with an RMS roughness of about 16 nm is most probably due to the manufacturing process. Extrusion-related surface defects have already been observed by Finch *et al.* [8]. These inhomogenities show up in the coated PET films because the very thin coatings are not able to smooth the microscale structure. As far as coating defects are concerned, some pinholes were observed on the coated PET films, most probably due to coated dust particles which were removed later [7]. Furthermore, we are convinced that the good adhesion of the hydrocarbon coatings on the substrate plays a crucial role in microcrack formation and permeation behaviour because the effective area of each microcrack is enhanced due to lateral diffusion of the gas in the polymer near the interface with the barrier coating. Permeability measurements on SiO_x-coated PET films indicate that peeled-off regions and pinholes in the barrier layer are responsible for their higher permeation data compared to the SiO_x-bulk value extrapolated to the same thickness [12].

5. Conclusions

These studies highlight some of the possibilities for improving polymer materials, with respect to gas and water vapour permeation, presented by plasma technology. Detailed evaluation of other possible plasma procedures, such as radiofrequency plasma processes with our reactor will enable us to find out the simplest, most effective and least costly way to arrive at our goal. New results will be presented in future reports.

Acknowledgements

The work was supported by the Swiss Foundation for Technology and Innovation under no. 2377.1. The authors are grateful to R. Urech for technical assistance, Dr Z. Harmati for measuring oxygen permeability, E. Furrer for carrying out water-vapour permeability measurements, Dr E. Hack for developing a technique to analyse the formation of microcracks, Dr D. Anselmetti, Novartis Services AG, and Dr H. Künzli for recording AFM images, and Dr S. Mikhailov and Dr J. Weber, Université de Neuchâtel, for performing RBS and ERD analysis.

References

1. J. RELLMANN and H. SCHENCK, *Kunststoffe* **82** (1992) 2.
2. J. E. KLEMBERG-SAPIEHA, L. MARTINU, O. M. KÜTTEL and M. R. WERTHEIMER, in "Proceedings of the 36th Annual Technical Conference on SVC," Dallas (1993) pp. 445–9.
3. H. CHATHAM, *Surf. Coat. Technol.* **78** (1996) 1.
4. Y. LIN and H. YASUDA, *J. Appl. Polym. Sci.* **60** (1996) 2227, and references therein.
5. J. F. FRIEDRICH, L. WIGANT, W. UNGER, A. LIPPITZ, H. WITTRICH, D. PRESCHER, J. ERDMANN, H.-V. GORSLER and L. NICK, *J. Adhes. Sci. Technol.* **9** (1995) 1165.
6. M. WALTHER, M. HEMING, and M. SPALLEK, *Surf. Coat. Technol.* **80** (1996) 200.
7. E. M. MOSER, R. URECH, E. HACK, H. KÜNZLI and E. MÜLLER, in "Proceedings of the 10th International Conference on Thin Films," Salamanca, September 1996, in press.
8. D. S. FINCH, J. FRANKS, N. X. RANDALL, A. BARNETSON, J. CROUCH, A. C. EVANS and B. RALPH, *Packag. Technol. Sci.* **9** (1996) 73.
9. E. HACK and E. M. MOSER, *J. Mater. Sci. Lett.*, submitted.
10. K. LANGE, Diss. Techn. Universität München (1995).
11. J. C. ANGUS, *Thin Solid Films* **142** (1986) 145.
12. K. KESSLER, Diss. ETH Nr. 10794, Zürich (1994).

Received 16 June 1997
and accepted 23 July 1998